Refined shell finite elements based on RMVT and MITC for the analysis of laminated structures

Refined shell finite elements based on RMVT and MITC for the analysis of laminated structures

Maria Cinefra[1], Claudia Chinosi[2], Lucia Della Croce[3]
[1]*Department of Mechanical and Aerospace Engineering, Politecnico di Torino, Italy*
E-mail: maria.cinefra@polito.it, erasmo.carrera@polito.it

[2]*Department of Science and Advanced Technologies, Universit del Piemonte Orientale, Italy*
E-mail: claudia.chinosi@mfn.unipmn.it

[3]*Department of Mathematics, Universit di Pavia, Italy*
E-mail: lucia.dellacroce@unipv.it

Keywords: Mixed Interpolated Tensorial Components, shell finite elements, Reissner's Mixed Variational Theorem, refined theories, sandwich, isotropic.

SUMMARY. In this paper, we present some advanced shell models for the analysis of multilayered structures in which the mechanical and physical properties may change in the thickness direction. The finite element method showed successful performances to approximate the solutions of the advanced structures. In this regard, two variational formulations are available to reach the stiffness matrices, the principle of virtual displacement (PVD) and the Reissner mixed variational theorem (RMVT). Here we introduce a strategy similar to MITC (Mixed Interpolated of Tensorial Components) approach, in the RMVT formulation, in order to construct an advanced locking-free finite element. Moreover, assuming the transverse stresses as independent variables, the continuity at the interfaces between layers is easily imposed. We show that in the RMVT context, the element exhibits both properties of convergence and robustness when comparing the numerical results with benchmark solutions from literature.

1 INTRODUCTION

Multilayered structures are increasingly used in many fields. Examples of multilayered structures are sandwich constructions, composite structures made of orthotropic laminae or layered structures made of different isotropic layers (such as those employed for thermal protection). In most of the applications, these structures mostly appear as flat (plates) or curved panels (shells). In this paper, attention has been restricted to flat structures made of different isotropic layers, although the models could be easily extended to other cases.

The analysis of multilayered structures is difficult when compared to one layered ones. A number of complicating effects arise when their mechanical behavior as well as failure mechanisms have to be correctly understood. This is due to the intrinsic discontinuity of the mechanical properties at each layer–interface to which high shear and normal transverse deformabilty is associated. An accurate description of the stress and strain fields of these structures requires theories that are able to satisfy the so–called Interlaminar Continuity (IC) conditions for the transverse stresses (see Whitney [1], and Pagano [2], as examples). Transverse anisotropy of multilayered structures make it difficult to find closed form solutions and the use of approximated solutions is necessary. It can therefore be concluded that the use of both refined two–dimensional theories and computational methods become mandatory to solve practical problems related to multilayered structures.

Among the several available computational methods, the Finite Element Method (FEM) has played

and continues to play a significant role. In this work, the Reissner's Variational Mixed Theorem (RMVT) is used to derive plate finite elements. As a main property, RMVT permits one to assume two independent fields for diplacement and transverse stress variables. The resulting advanced finite elements therefore describe *a priori* interlaminar continuous transverse stress fields.

For a complete and rigorous understanding of the foundations of RMVT, reference can be made to the articles by Professor Reissner [3]-[5] and the review article by Carrera [6]. The first application of RMVT to modeling of multilayered flat structures was performed by Murakami [7],[8]. He introduced a first order displacement field in his papers, in conjunction with an independent parabolic transverse stress LW field in each layer (transverse normal stress and strain were discarded). An extension to a higher order displacement field was proposed by Toledano and Murakami in [9]. While in [10], they extended the RMVT to a layer-wise description of both displacement and transverse stress fields. These papers [7]-[10] should be considered as the fundamental works in the applications of RMVT as a tool to model multilayered structures. Further discussions on RMVT were provided by Soldatos [11]. A generalization, proposing a systematic use of RMVT as a tool to furnish a class of two dimensional theories for multilayered plate analysis, was presented by Carrera [12],[13]. The order of displacement fields in the layer was taken as a free parameter of the theories. Applications of what is reported in [12],[13] have been given in several other papers [14]-[21], in which closed-form solution are considered. Layer-wise mixed analyses were performed in [22] for the static case. As a fundamental result, the numerical analysis demonstrated that RMVT furnishes a quasi three-dimensional a priori description of transverse stresses, including transverse normal components. Sandwich plates were also considered in [15]. Recently, Messina [23] has compared RMVT results to PVD (Principle of Virtual Displacements) ones. Transverse normal stresses were, however, discarded in this work.
In [24]-[26], Carrera and Demasi developed multilayered plate elements based on RMVT, that were able to give a quasi–three-dimensional description of stress/strain fields. But in these works, they still employ the selective reduced integration [27] to overcome the shear locking phenomenon.

Recently, authors adopted the Mixed Interpolation of Tensorial Components (MITC) to contrast the locking. According to this technique, the strain components are not directly computed from the displacements but they are interpolated within each element using a specific interpolation strategy for each component. For more details about MITC, the readers can refer to the works [28]-[32]. In [33] and [34], the authors formulated plate/shell elements based on displacement formulation that showed good properties of convergence thanks to the use of the MITC. The idea of this work is to interpolate the transverse stresses (that are modelled a-priori by the RMVT) using the same strategy of the MITC. In this way, the RMVT permits both to satisfy IC conditions and to withstand the shear locking.

The shell elements here proposed have nine nodes. The displacement field and transverse fields are defined according to the Unified Formulation [35] introduced by Carrera. In particular, higher-order layer-wise models are used for the analysis of multilayered structures. The shear stresses σ_{xz} and σ_{yz} are interpolated in each element according to the MITC in order to contrast the shear locking. Also the in-plane strains are re-interpolated in order to withstand the membrane locking. Comparisons with 3D solutions are provided and they demonstrate the efficiency of elements presented.

2 THE MODEL

2.1 *Reissner's Mixed Variational Theorem*

The stress vector $\boldsymbol{\sigma} = (\sigma_i),\ \ i = 1, ...6$ can be written in terms of the in-plane and transverse components as $\boldsymbol{\sigma} = [\boldsymbol{\sigma}_p\ \ \boldsymbol{\sigma}_n]$ with:

$$\boldsymbol{\sigma}_p = [\sigma_{\alpha\alpha}\ \sigma_{\beta\beta}\ \sigma_{\alpha\beta}]^T,\ \ \boldsymbol{\sigma}_n = [\sigma_{\alpha z}\ \sigma_{\beta z}\ \sigma_{zz}]^T \tag{1}$$

and analogously the strain vector $\boldsymbol{\epsilon} = (\epsilon_i)$, $i = 1, ...6$ can be written in terms of the in-plane and transverse components as $\boldsymbol{\epsilon} = [\boldsymbol{\epsilon}_p\ \boldsymbol{\epsilon}_n]$, with:

$$\boldsymbol{\epsilon}_p = [\epsilon_{\alpha\alpha}\ \epsilon_{\beta\beta}\ \epsilon_{\alpha\beta}]^T,\ \ \boldsymbol{\epsilon}_n = [\epsilon_{\alpha z}\ \epsilon_{\beta z}\ \epsilon_{zz}]^T \tag{2}$$

The PVD variational equation is written as:

$$\int_V (\delta\boldsymbol{\epsilon}_{pG}^T\boldsymbol{\sigma}_{pH}\ +\ \delta\boldsymbol{\epsilon}_{nG}^T\boldsymbol{\sigma}_{nH})dV\ =\ \delta L_e \tag{3}$$

The subscript H means that the stresses are computed by Hooke's law, while the subscript G means that the strains are computed from geometrical relations. The superscript T stands for transposition operation, V represents the 3D multilayered body volume. δL_e is the virtual variation of the work.

In the RMVT formulation the transverse stresses are assumed as independent variables and denoted by $\boldsymbol{\sigma}_{nM}$ (M stands for *Model*). The transverse strains are evaluated by Hooke's law and denoted by $\boldsymbol{\epsilon}_{nH}$. They should be related to the geometrical strains $\boldsymbol{\epsilon}_{nG}$ by the constraint equation:

$$\boldsymbol{\epsilon}_{nH} = \boldsymbol{\epsilon}_{nG}. \tag{4}$$

By adding in (3) the compatibility condition (4) through a Lagrange multipliers field, which turn out to be transverse stresses, one then obtain the RMVT formulation:

$$\begin{aligned}\int_V (\delta\boldsymbol{\epsilon}_{pG}^T\boldsymbol{\sigma}_{pH} + \delta\boldsymbol{\epsilon}_{nG}^T\boldsymbol{\sigma}_{nM} + \delta\boldsymbol{\sigma}_{nM}^T(\boldsymbol{\epsilon}_{nG} - \boldsymbol{\epsilon}_{nH}))dV \\ = \delta L_e\end{aligned} \tag{5}$$

The third 'mixed' term variationally enforces the compatibility of the transverse strain components.

2.2 *The constitutive equations and the geometrical relations*

In this section we will explain in detail the construction of RMVT employing the Hooke's law and the geometrical relations (see for example [25],[26]).

Referring to the Hooke's law for orthotropic material $\sigma_i = \tilde{C}_{ij}\epsilon_j,\ i, j = 1, ...6$ the constitutive equations become:

$$\begin{aligned}\boldsymbol{\sigma}_{pH} &= \tilde{\mathbf{C}}_{pp}\boldsymbol{\epsilon}_{pG} + \tilde{\mathbf{C}}_{pn}\boldsymbol{\epsilon}_{nG} \\ \boldsymbol{\sigma}_{nH} &= \tilde{\mathbf{C}}_{np}\boldsymbol{\epsilon}_{pG} + \tilde{\mathbf{C}}_{nn}\boldsymbol{\epsilon}_{nG}\end{aligned} \tag{6}$$

where the material matrices are:

$$\tilde{\mathbf{C}}_{pp} = \begin{bmatrix} \tilde{C}_{11} & \tilde{C}_{12} & \tilde{C}_{16} \\ \tilde{C}_{12} & \tilde{C}_{22} & \tilde{C}_{26} \\ \tilde{C}_{16} & \tilde{C}_{26} & \tilde{C}_{66} \end{bmatrix} \quad \tilde{\mathbf{C}}_{pn} = \begin{bmatrix} 0 & 0 & \tilde{C}_{13} \\ 0 & 0 & \tilde{C}_{23} \\ 0 & 0 & \tilde{C}_{36} \end{bmatrix}$$
$$\tilde{\mathbf{C}}_{np} = \tilde{\mathbf{C}}_{pn}^{T}; \quad \tilde{\mathbf{C}}_{nn} = \begin{bmatrix} \tilde{C}_{55} & \tilde{C}_{45} & 0 \\ \tilde{C}_{45} & \tilde{C}_{44} & 0 \\ 0 & 0 & \tilde{C}_{33} \end{bmatrix} \tag{7}$$

The weak form of Hooke's law according to the RMVT is:

$$\begin{aligned} \boldsymbol{\sigma}_{pH} &= \mathbf{C}_{pp}\boldsymbol{\epsilon}_{pG} + \mathbf{C}_{pn}\boldsymbol{\sigma}_{nM} \\ \boldsymbol{\epsilon}_{nH} &= \mathbf{C}_{np}\boldsymbol{\epsilon}_{pG} + \mathbf{C}_{nn}\boldsymbol{\sigma}_{nM} \end{aligned} \tag{8}$$

where:

$$\begin{aligned} \mathbf{C}_{pp} &= [\tilde{\mathbf{C}}_{pp} - \tilde{\mathbf{C}}_{pn}(\tilde{\mathbf{C}}_{nn})^{-1}\tilde{\mathbf{C}}_{np}] \\ \mathbf{C}_{pn} &= \tilde{\mathbf{C}}_{pn}(\tilde{\mathbf{C}}_{nn})^{-1} \\ \mathbf{C}_{np} &= -(\tilde{\mathbf{C}}_{nn})^{-1}\tilde{\mathbf{C}}_{np} \\ \mathbf{C}_{nn} &= (\tilde{\mathbf{C}}_{nn})^{-1} \end{aligned} \tag{9}$$

and $\boldsymbol{\sigma}_{nM}$ are the independent variables of our mode.

By considering a shell with constant radii of curvature and naming the curvilinear reference system as (α, β, z), the geometrical relations can be written in matrix form as:

$$\begin{aligned} \boldsymbol{\varepsilon}_p &= [\varepsilon_{\alpha\alpha}, \varepsilon_{\beta\beta}, \varepsilon_{\alpha\beta}] = (\boldsymbol{D}_p + \boldsymbol{A}_p)\boldsymbol{u}\,, \\ \boldsymbol{\varepsilon}_n &= [\varepsilon_{\alpha z}, \varepsilon_{\beta z}, \varepsilon_{zz}] = (\boldsymbol{D}_{np} + \boldsymbol{D}_{nz} - \boldsymbol{A}_n)\boldsymbol{u}\,, \end{aligned} \tag{10}$$

where $\mathbf{u} = [u\ v\ w]$ and the differential operators are:

$$\boldsymbol{D}_p = \begin{bmatrix} \frac{\partial_\alpha}{H_\alpha} & 0 & 0 \\ 0 & \frac{\partial_\beta}{H_\beta} & 0 \\ \frac{\partial_\beta}{H_\beta} & \frac{\partial_\alpha}{H_\alpha} & 0 \end{bmatrix}, \quad \boldsymbol{D}_{np} = \begin{bmatrix} 0 & 0 & \frac{\partial_\alpha}{H_\alpha} \\ 0 & 0 & \frac{\partial_\beta}{H_\beta} \\ 0 & 0 & 0 \end{bmatrix}, \quad \boldsymbol{D}_{nz} = \begin{bmatrix} \partial_z & 0 & 0 \\ 0 & \partial_z & 0 \\ 0 & 0 & \partial_z \end{bmatrix}, \tag{11}$$

$$\boldsymbol{A}_p = \begin{bmatrix} 0 & 0 & \frac{1}{H_\alpha R_\alpha} \\ 0 & 0 & \frac{1}{H_\beta R_\beta} \\ 0 & 0 & 0 \end{bmatrix}, \boldsymbol{A}_n = \begin{bmatrix} \frac{1}{H_\alpha R_\alpha} & 0 & 0 \\ 0 & \frac{1}{H_\beta R_\beta} & 0 \\ 0 & 0 & 0 \end{bmatrix}. \tag{12}$$

In these arrays, the metric coefficients are:

$$H_\alpha = (1 + z/R_\alpha)\,, \quad H_\beta = (1 + z/R_\beta)\,, \quad H_z = 1\,. \tag{13}$$

where R_α and R_β are the principal radii of curvature along the coordinates α and β, respectively.

In RMVT the compatibility condition of the transverse strains is enforced by equating the second equation of (8) with second equation of (10).

2.3 *Mixed Interpolated Tensorial Components*

According to the finite element method and considering a nine-nodes element, the displacement components and their virtual variations are interpolated on the nodes of the element by means of the classical Lagrangian shape functions N_i:

$$\boldsymbol{u} = N_i \delta \boldsymbol{q}_i \qquad \text{with} \quad i = 1, ..., 9 \tag{14}$$

where $\boldsymbol{q}_j$ and $\delta \boldsymbol{q}_i$ are the nodal displacements and their virtual variations.
Considering the local coordinate system (ξ, η) of the element, the MITC shell elements ([36],[37]) are formulated by using, instead of the strain components directly computed from the displacements, an interpolation of these within each element using a specific interpolation strategy for each component. The corresponding interpolation points, called tying points, are shown in figure 1 for a nine-nodes element.
The interpolating functions are calculated by imposing that the function assumes the value 1 in the corresponding tying point and 0 in the others. These are arranged in the following arrays:

$$\begin{aligned} \bar{N}_1 &= [N_{A1}, N_{B1}, N_{C1}, N_{D1}, N_{E1}, N_{F1}] \\ \bar{N}_2 &= [N_{A2}, N_{B2}, N_{C2}, N_{D2}, N_{E2}, N_{F2}] \\ \bar{N}_3 &= [N_P, N_Q, N_R, N_S] \end{aligned} \tag{15}$$

Therefore, the in-plane strain components and the shear stresses are interpolated as follows:

$$\varepsilon_{\alpha\alpha} = \bar{N}_{1_m} \varepsilon_{\alpha\alpha_m} \; ; \quad \varepsilon_{\beta\beta} = \bar{N}_{2_m} \varepsilon_{\beta\beta_m} \; ; \quad \varepsilon_{\alpha\beta} = \bar{N}_{3_m} \varepsilon_{\alpha\beta_m} \tag{16}$$

$$\sigma_{\alpha z} = \bar{N}_{1_m} \sigma_{\alpha z_m} \quad \sigma_{\beta z} = \bar{N}_{2_m} \sigma_{\beta z_m} \tag{17}$$

with $m = 1, \ldots, 6$, except $\varepsilon_{\alpha\beta}$ for which $m = 1, \ldots, 4$. The strain components $\varepsilon_{\alpha\alpha_m}$, $\varepsilon_{\beta\beta_m}$ and $\varepsilon_{\alpha\beta_m}$ still depend on displacements (14) by means of geometrical relations (10) and the shape functions N_i are evaluated in the tying points.
Note that the transverse normal stress σ_{zz} is excluded from this procedure because it doesn't produce locking and it is interpolated on the standard nodes of the element as the displacements:

$$\sigma_{zz} = N_i \sigma_{zz_i} \qquad \text{with} \quad i = 1, \ldots, 9 \tag{18}$$

2.4 *Unified Formulation*

The main feature of the Unified Formulation by Carrera [35] (CUF) is the unified manner in which the variables are handled. According to CUF, the displacement field and the transverse stress field are written by means of approximating functions in the thickness direction as follows:

$$\boldsymbol{u}^k(\alpha,\beta,z) = F_\tau(z)\boldsymbol{u}^k_\tau(\alpha,\beta)\,; \quad \boldsymbol{\sigma}^k_n(\alpha,\beta,z) = F_\tau(z)\boldsymbol{\sigma}^k_{n_\tau}(\alpha,\beta) \qquad \tau = 0,1,...,N \tag{19}$$

where F_τ are the so-called thickness functions depending only on the coordinate z. $\boldsymbol{u}_\tau$, σ_{n_τ} are the unknown variables depending on the in-plane coordinates α,β and they are approximated by FEM. τ is a sum indexes and N is the order of expansion assumed in the thickness direction (usually $N = 1,...,4$).

If one chooses to adopt a Layer-Wise (LW) approach, the variables are defined independently for each layer k of the multilayer as follows:

$$\boldsymbol{u}^k = F_t\,\boldsymbol{u}^k_t + F_b\,\boldsymbol{u}^k_b + F_r\,\boldsymbol{u}^k_r = F_\tau\,\boldsymbol{u}^k_\tau, \qquad \tau = t,b,r\,, \quad r = 2,...,N. \tag{20}$$

$$\boldsymbol{\sigma}^k_n = F_t\,\boldsymbol{\sigma}^k_{n_t} + F_b\,\boldsymbol{\sigma}^k_{n_b} + F_r\,\boldsymbol{\sigma}^k_{n_r} = F_\tau\,\boldsymbol{\sigma}^k_{n_\tau}, \qquad \tau = t,b,r\,, \quad r = 2,...,N. \tag{21}$$

$$F_t = \frac{P_0+P_1}{2}, \quad F_b = \frac{P_0-P_1}{2}, \quad F_r = P_r - P_{r-2}. \tag{22}$$

in which $P_j = P_j(\zeta_k)$ is the Legendre polynomial of j-order defined in the ζ_k-domain: $-1 \leqslant \zeta_k \leqslant 1$.
In this way, the top (t) and bottom (b) values of the displacements and stresses are used as unknown variables and one can impose the following compatibility conditions:

$$\boldsymbol{u}^k_t = \boldsymbol{u}^{k+1}_b\,, \quad \boldsymbol{\sigma}^k_{n_t} = \boldsymbol{\sigma}^{k+1}_{n_b}\,, \qquad k = 1, N_l - 1 \tag{23}$$

From this point on, the models here presented will be indicated as LMN (L=layer-wise and M=mixed), where N is the order of expansion assumed in the thickness direction.

3 NUMERICAL RESULTS

In order to present the performance of our element, we have considered two tests: a sandwich plate with isotropic core and skins (see [38]) and a cylinder (see Figure 2) of the same material. These structures are simply supported and they are loaded with a bisinusoidal distribution of transverse pressure applied to the top surface of the multilayer:

$$p(\alpha,\beta) = \sin\left(\frac{\pi\alpha}{a}\right)\sin\left(\frac{\pi\beta}{b}\right)$$

where L is used in place of a for the cylinder. The wave numbers are: $m = n = 1$ for the plate and $m = 1$, $n = 8$ for the cylinder.
The elastic and geometrical properties are reported in Table 1, where a, b are the in-plane dimensions of the plate and R is the radius of the mid-surface of the cylinder.

We compare the results obtained with our finite element models with the analytical solution obtained with a LM4 model and the Navier method (see [38]). This can be considered a quasi-3D solution. Furthermore to validate the improvement of the solution approximated by the mixed models in respect to classical models, we present the comparison with First-order Shear Deformation Theory model (FSDT) in some cases. A mesh 10×10 is used to perform the analysis of the plate, while 10×20 (20 in the circumferential direction) elements are taken for the cylinder. This choice ensures the convergence of the solution.

The normalized transverse displacement $\bar{w}$ is evaluated at $z = 0$ in correspondence of the maximum of the load:

$$\bar{w} = w(z = 0)\frac{100E_c}{h(\frac{a}{h})^4}$$

For the cylinder, R/h is considered in place of a/h.

The results are provided in Table 2 and 3 for the plate and the cylinder, respectively. As expected, the FSDT and the LMN models give the same results in the case of thin plate ($a/h = 100$), while for the thick plate ($a/h = 1$) mixed models with high orders of expansion are necessary in order to match the quasi-3D solution. The Table 2 shows also that the mixed models here presented lead to a locking-free finite element to treat the multilayered plates. The normalized transverse displacement confirms the performance and the robustness of the element even for very thin sandwich plates. The same conclusion can be drawn from Table 3 for the cylinder.
In Figures 3 and 4, we report the distribution of shear stress $\sigma_{\alpha z}$ and the normal stress σ_{zz} along the thickness of the plate and the cylinder, respectively. They are evaluated in the points of the domain where they assume maximum values. It is evident the non-linear distribution of the shear and normal stresses obtained by high-order mixed models. In particular, one can note that LMN models permit to satisfy the interlaminar continuity conditions even if the plate/cylinder is very thick ($a/h = 1, R/h = 4$) and the mechanical properties between layers are very different ($E_{skin}/E_{core} = 50$).

4 CONCLUSIONS

In this work an advanced locking-free finite element for the analysis of the multilayered structures has been presented. The problem is modelled by adopting the variational formulation based on RMVT. Mixed theories with layerwise (LW) description of both the displacements and the transverse stresses are formulated. Different orders of expansion of variables in the thickness directions are considered. The continuity condition of the transverse stresses at the interfaces between layers (IC) is easily imposed by assuming the stresses as independent variables. The in-plane approximation is performed by a strategy similar to MITC (Mixed Interpolated Tensorial Components) finite element approach. Two tests of simply supported sandwich plate and cylinder with isotropic core and skins are considered in order to validate both properties of convergence and robusteness of the element. The comparison with the quasi-3D solution shows an improvement of the behaviour of the solution as regards both the description of transverse displacement and the transverse stresses. The analysis of the solutions, performed versus the thickness of the structure, confirms that the elements presented are locking-free for very thin structures. Moreover, these advanced elements permit the transverse stresses to be correctly described along the thickness even when the multilayered structure is very thick and the properties between layers are very different. More results about the analysis of multilayered shell composite structures will be provided in future companion works.

References

[1] Whitney, J.M., "The effects of transverse shear deformation on the bending of laminated plates," *J. Compos. Mat.*, **3**, 534-547, (1969).

[2] Pagano, N.J., "Exact solutions for Composite Laminates in Cylindrical Bending," *J. Compos. Mat.*, **3**, 398-411, (1969).

[3] Reissner, E., "On a certain mixed variational theory and a proposed application," *Int. J. Numer. Meth. Eng.*, **20**, 13661368, (1984).

[4] Reissner, E., "On a mixed variational theorem and on a shear deformable plate theory," *Int. J. Numer. Meth. Eng.*, **23**, 193198, (1986).

[5] Reissner, E., "On a certain mixed variational theorem and on a laminated elastic shell theory," *Proc. of Euromech-Colloquium*, **219**, 1727, (1986).

[6] Carrera, E., "Developments, ideas, and evaluations based upon Reissners Mixed Variational Theorem in the modeling of multilayered plates and shells," *Appl. Mech. Rev.*, **54**(4), 301329, (2001).

[7] Murakami, H., "Laminated composite plate theory with improved in-plane responses," *ASME Proc. of PVP Conf., New Orleans*, **98**(2), 257263, (1985).

[8] Murakami, H., "Laminated composite plate theory with improved in-plane responses," *ASME J. Appl. Mech.*, **53**, 661666, (1986).

[9] Toledano, A. and Murakami, H., "A high-order laminated plate theory with improved in-plane responses," *Int. J. Solids Struct.*, **23**, 111131, (1987).

[10] Toledano, A. and Murakami, H., "A composite plate theory for arbitrary laminate configurations," *ASME J. Appl. Mech.*, **54**, 181189, (1987).

[11] Soldatos, K.P., "Cylindrical bending of cross-ply laminated plates: refined 2D plate theories in comparison with the exact 3D elasticity solution," Tech. Report 140, Dept. of Math., University of Ioannina, Greece.

[12] Carrera, E., "A class of two-dimensional theories for anisotropic multilayered plates analysis," *Accademia delle Scienze di Torino, Memorie Scienze Fisiche*, **19-20**, 139, (1995).

[13] Carrera, E., "C_0^z Requirements-models for the two dimensional analysis of multilayered structures," *Compos. Struct.*, **37**, 373384, (1997).

[14] Carrera, E., "A Reissner's mixed variational theorem applied to vibration analysis of multilayered shells," *ASME J. Appl. Mech.*, **66**, 6978, (1999).

[15] Carrera, E., "Mixed layer-wise models for multilayered plates analysis," *Compos. Struct.*, **43**, 5770, (1998).

[16] Carrera, E., "Evaluation of layer-wise mixed theories for laminated plates analysis," *AIAA J.*, **26**, 830839, (1998).

[17] Carrera, E., "Transverse normal stress effects in multilayered plates," *ASME J. Appl. Mech.*, **66**, 10041012, (1999).

[18] Carrera, E., "A study of transverse normal stress effects on vibration of multilayered plates and shells," *J. Sound Vib.* **225**, 803-829, (1999).

[19] Carrera, E., "Single-layer vs multi-layers plate modelings on the basis of Reissners mixed theorem," *AIAA J.*, **38**(2), 342352, (2000).

[20] Carrera, E., "A priori vs a posteriori evaluation of transverse stresses in multilayered orthotropic plates," *Compos. Struct.*, **48**, 245-260, (2000).

[21] Carrera, E., "Vibrations of layered plates and shells via Reissner's Mixed Variational Theorem," In: *Fourth Symposiom on Vibrations of Continuos Systems*, Kenswick, 2003, July 7-11, 4-6.

[22] Carrera, E., "Layer-wise mixed models for accurate vibration analysis of multilayered plates," *ASME J. Appl. Mech.*, **65**, 820828, (1998).

[23] Messina, A., "Two generalized higher order theories in free vibration studies of multilayered plates," *J. Sound Vib.* **242**, 125150, (2001).

[24] Carrera, E. and Demasi, L., "Sandwich plates analyses by finite element method and Reissner's Mixed Theorem," In: *Sandwich V, Zurich*, 2000, September 5-7, 301-313.

[25] Carrera, E. and Demasi, L., "Multilayered finite plate element based on Reissner Mixed Variational Theorem. Part I: Theory," *Int. J. Numer. Meth. Eng.* **55**, 191-231, (2002).

[26] Carrera, E. and Demasi, L., "Multilayered finite plate element based on Reissner Mixed Variational Theorem. Part II: Numerical Analysis," *Int. J. Numer. Meth. Eng.*, **55**, 253-296, (2002).

[27] Zienkiewicz, O.C., Taylor, R.L. and Too, J.M., "Reduced integration techniques in general analysis of plates and shells," *Int. J. Numer. Meth. Eng.*, **3**, 275-290, (1971).

[28] Huang, H.-C., "Membrane locking and assumed strain shell elements," *Comput. Struct.*, **27**(5), 671-677, (1987).

[29] Brezzi, F., Bathe, K.-J. and Fortin, M., "Mixed-interpolated elements for Reissner-Mindlin plates," *Int. J. Numer. Meth. Eng.*, **28**, 1787-1801, (1989).

[30] Chinosi, C. and Della Croce, L., "Mixed-interpolated elements for thin shell," *Commun. Numer. Meth. Eng.*, **14**, 1155-1170, (1998).

[31] Bathe, K.-J., Lee, P.-S. and Hiller, J.-F., "Towards improving the MITC9 shell element," *Comput. Struct.* **81**, 477-489, (2003).

[32] Panasz, P. and Wisniewski, K., "Nine-node shell elements with 6 dofs/node based on two-level approximations. Part I Theory and linear tests," *Fin. Elem. Anal. Design*, **44**, 784-796, (2008).

[33] Cinefra, M., Chinosi, C. and Della Croce, L., "MITC9 shell elements based on refined theories for the analysis of isotropic cylindrical structures," *Mech. Adv. Mater. Struct.*, **20**, 91-100, (2013).

[34] Cinefra, M. and Carrera, E., "Shell finite elements with different through-the-thickness kinematics for the linear analysis of cylindrical multilayered structures," *Int. J. Numer. Meth. Eng.*, **93**, 160-182, (2013).

[35] Carrera, E., "Theories and finite elements for multilayered, anisotropic, composite plates and shells," *Arch. Comput. Meth. Engng.*, **9**(2), 87-140, (2002).

[36] Bathe, K.-J. and Dvorkin, E., "A formulation of general shell elements - the use of mixed interpolation of tensorial components," *Int. J. Numer. Meth. Eng.*, **22**, 697-722, (1986).

[37] Bucalem, M.L. and Bathe, K.-J., "Higher-order MITC general shell elements," *Int. J. Numer. Meth. Eng.*, **36**, 3729-3754, (1993).

[38] Carrera, E. and Brischetto, S., "A survey with numerical assessment of classical and refined theories for the analysis of sandwich plates," *Appl. Mech. Rev.*, **62**(1), 010803(17 pages), (2009).

Table 1: Elastic and geometrical properties of sandwich.

Properties	Skins	Core
E(GPa)	50	1
ν	0.25	0.25
G(GPa)	20	0.4
h(m)	0.1	0.8
b=3a(m)	3,300	
R(m)	10	

Table 2: Plate. Maximum normalized transversal displacement $\bar{w}$.

$\bar{w}$	$a/t = 1$	$a/t = 100$
quasi-3D [38]	15.05	0.3778
FSDT	2.486	0.3757
LM1	18.23	0.3768
LM2	15.30	0.3768
LM3	15.07	0.3759
LM4	15.04	0.3768

Tables

Table 3: Cylinder. Maximum normalized transversal displacement $\bar{w}$.

$\bar{w}$	$R/h = 4$	$R/h = 100$	$R/h = 1000$
quasi-3D	6.588	0.7389	0.0327
LM2	6.586	0.7388	0.0328
LM4	6.585	0.7388	0.0328

Figures

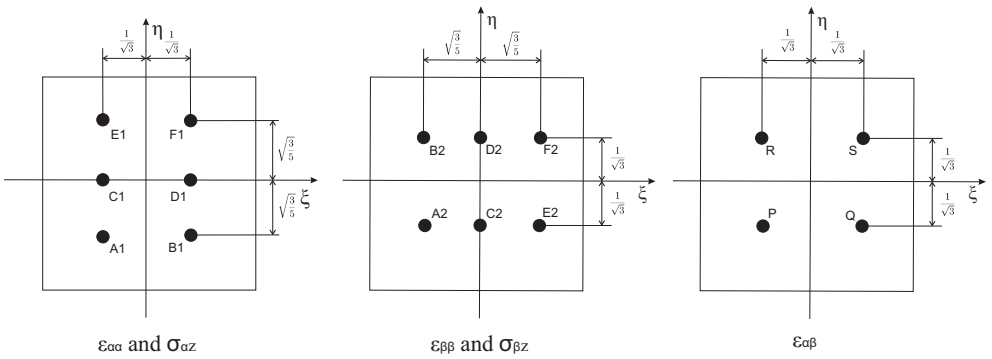

Figure 1: Tying points for the MITC9 shell finite element.

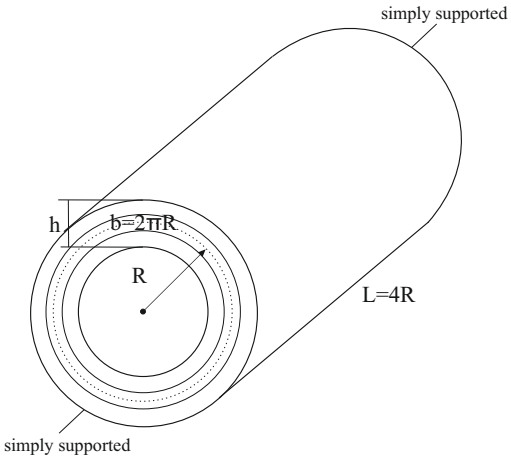

Figure 2: Geometry of the cylinder.

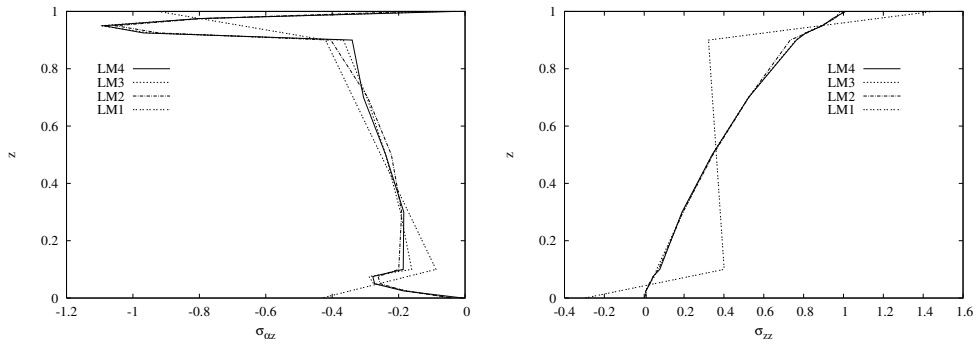

(a) Shear stress. (b) Normal stress.

Figure 3: Distributions od transverse stresses along the thickness in the very thick plate ($a/h = 1$).

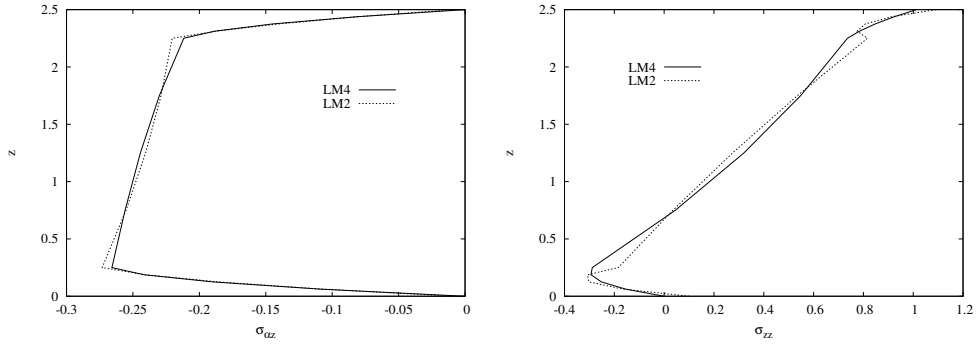

(a) Shear stress. (b) Normal stress.

Figure 4: Distributions od transverse stresses along the thickness in the very thick cylinder ($R/h = 4$).